doi: 10.5028/jatm.2012.04014911

Characterization of Surface Level Wind in the Centro de Lançamento de Alcântara for Use in Rocket Structure Loading and Dispersion Studies

Edson R. Marciotto*, Gilberto Fisch, Luiz E. Medeiros
Instituto de Aeronáutica e Espaço / São José dos Campos/SP - Brazil

Abstract: *We present wind data collected for ten days during the dry season in 2008 during the Murici II Campaign, which was carried out in the area of the Centro de Lançamento de Alcântara (CLA). The main goals are to better understand processes governing the wind regime in the CLA and the development of tools for analyzing the impact of wind on rocket structure and on the dispersion of pollutants released during the launch. A set of 11 aerovanes (ten at 10-m height and one at 1.5-m height) plus a sonic anemometer at 1.5-m height were deployed to measure wind speed and direction, which were stored as ten-minute data. Turbulence intensity, gust factor, and gust amplitude were computed from the available dataset. Statistical analysis shows that the wind direction is predominant from East-Northeast (ENE), with the mean vector wind direction of 60º, in agreement with the trade wind regime. The diurnal cycle of all statistical properties of the wind are strongly marked. Wind speed, turbulence intensity, and gusts are peaked at about 1000 LST. The presence of a non-diurnal cycle of four days has been noticed and might be associated with synoptic systems acting on the region. A simple heuristic formula was proposed to compute Lagrangian time-scale from Eulerian time-scale, and from which we compute the Lagragian standard deviation, a final product to be used as input in diffusion models.*

Keywords: *Centro de Lançamento de Alcântara, Surface Wind, Rocket Load, Plume Dispersion.*

INTRODUCTION

Brazilian rockets are launched from Centro de Lançamento de Alcântara (CLA), whose location close to equator is privileged for launching geosynchronous satellites. Turbulence and sudden change of wind velocity may affect straightforward rockets' structure as well as its flight trajectory. The atmospheric boundary layer, the nearest atmospheric layer from surface, is the one with higher time and space variability. Furthermore, the geographic and topographic features around make the CLA a special case from the micrometeorological point of view, as it is located in the Atlantic Ocean sea board nearby a cliff about 40-m high. Detailed numerical simulations of a flow passing such a cliff have already been done by Pires *et al*. (2009).

Surface winds and turbulence in the atmospheric boundary layer govern the forces experienced by rockets in the first few seconds of the flight. Also, when there is only a very small clearance between the rocket and the launch tower winds, it can cause unaccepted tilts. Immediately before the launch, the rocket is taken from the tower shelter (Mobile Integration Tower) being exposed to the wind again (Kingwell *et al*., 1991). Thus, not only the rockets' launch is of concern of the aerospace meteorology, but also the maintenance of rockets in the launch pad. Following Kingwell *et al*. (1991), the wind factors influencing the rocket launch are, among others, flight trajectory, vehicle controllability, structural loadings on vehicle and towers, rate of salt deposition (and therefore of corrosion) on launch structures, and human and environmental protection.

Ground wind studies have been carried out by NASA concerning a safety environment for both launch procedures and dispersion of toxic gases and particulate matter rising from fuel burning (Adelfang *et al*., 2008). Rocket fuels produce gases of varying toxicity degrees. Generally, weather conditions such as entrainment of clear air and vertical mixing must be appropriate to keep concentrations of the combustion releases within the thresholds of toxicity. In this connection,

Received: 17/10/11. Accepted: 05/12/11
*author for correspondence: e.r.marciotto@gmail.com - Pç. Mal. Eduardo Gomes, 50. CEP: 12.228-901 - São José dos Campos/SP Brazil

Moreira *et al*. (2011) have developed a multi-layer model to simulate rocket's fuel-burning releases. Note that turbulence can be very critical in a go/no go decision: concomitantly to its desired effect on pollutants released during the fuel burning, there is an undesired effect on the structure of the rocket.

The importance of the wind profiles for vehicle launch has also been pointed out by Decker and Leach (2005) and Decker and Barbré (2011), who have been used wind profiles as input to a computer code to generate and validate vehicle steering commands to alleviate loads on the vehicle during ascent phase of missions in connection with NASA program. In particular, with respect to the intensity of the wind in the CLA, Fisch (1999) has studied the vertical profile of the wind in CLA and provided the first calculation of turbulence and gusts there. In a recent study, Fisch (2010) has compared two different sensors (aerovane and sonic anemometer) by analyzing the mean difference of wind speed and maximum wind speed. That study aimed at contributing to a better understanding of the wind time-series as they are obtained by aerovane or sonic anemometer, in order that the modernization of the wind data at the CLA could preserve their homogeneity for climatological purposes. A more detailed study of turbulent properties of the wind around the CLA has been addressed by Magnago *et al*. (2010), who used data of August, in 1999 (beginning of dry season), to calculate the spectrum of *u*, *v*, and *w* wind components and the ratios σ_u/u_*, σ_v/u_*, and σ_w/u_*; all these parameters are relevant to characterize the surface layer flow. A wider range of data covering five years (from 1995 to 1999) from a 70-m high anemometric tower was used by Gisler *et al*. (2011) for statistical analysis. Those studies have helped to construct a wind climatology of the CLA.

Nevertheless, they do not address the use of those data for practical/operational purposes. Therefore, many questions are still open and have to be answered. For example, what is the wind profile nearby the launch pad and how does it change from ocean upstream passing by the cliff? What are the concerning characteristics of turbulence and gusts, spatial distribution, and time scales for launching a rocket? Besides questions related to the launch safety, there are still problems of the safety of the population living in the neighborhood (Alcântara Town). Then, atmospheric data can be used to verify dispersion conditions of the boundary layer. One way to do it is by means of the computation of dispersion parameters served as input to numerical models, such as the Gaussian plume. The present study has also addressed this problem. Thus, the characterization of the surface boundary layer and, particularly, the internal boundary layer, is very important. In order to investigate these points, we present data of wind turbulence and gusts collected for ten days during the dry season in 2008, in the CLA.

SITE AND DATA

The CLA is located at the geographic coordinates 02°19'05" N; 44°22'04" W. In this latitude, wind trades interact with the sea breeze circulation, strengthening the easterly wind during the day (Gisler *et al*., 2011). The launch pad is located about 150m from the sea cost, and at the edge of sea-land there is a cliff about 40-m high (Fig. 1). The data analyzed here come from an aerovane mesh at 10-m high and from another couple of aerovanes (sonic and aerovane) 1.5-m high installed in this site.

Figure 1. The 40-m high cliff upwind the *Centro de Lançamento de Alcântara.*

Aerovane mesh

The data presented here were collected during the Murici II Campaign, in September 2008 from 16 to 25 (DOYs 260 to 269), corresponding to the local dry season. Synoptic conditions were fair with clear sky and no precipitation during the whole campaign. This experiment deployed, among other anemometers, ten aerovanes (model 05103 from R.M. Young) were displayed in a triangular mesh of masts 10-m high, and spaced 10-m from each other. Wind speed and direction were sampled at 0.5-Hz rate. Time-series of raw data were averaged over a ten-minute time interval and stored in a data-logger CR-7 Campbell Scientific Instrument. Figure 2 shows the layout of the aerovane mast mesh. The background of figure shows approximately the West view of the site so that the prevalent wind direction enters the page. Direct observations are: wind speed as given by the rotation rate of the aerovane

Figure 2. Site studied and the mast mesh layout. The view is of West portion of the site. Roughly speaking, the Trades are entering the page.

propeller after calibration applied, and wind direction, given by the aerovane potentiometer. The aerovanes were calibrated before and after the experiment in a wind tunnel in the Aerodynamics Division at Institute of Aeronautics and Space (IAE) using a Pitot tube as standard, not showing any tendency.

The zonal (u) and meridional (v) components of the wind velocity were computed from instantaneous values of the observed wind speed and direction. The vector mean wind speed was computed from mean components. Table 1 provides a summary of the calculation procedures. Aerovane direction in those formulas has been set with respect of the magnetic North, therefore a correction for magnetic declination had to be applied. The new vector mean wind direction speed and new vector mean wind speed are written as Eq. 1:

$$\begin{pmatrix} \bar{u}' \\ \bar{v}' \end{pmatrix} = \begin{pmatrix} -\cos\delta & -\sin\delta \\ \sin\delta & -\cos\delta \end{pmatrix} \begin{pmatrix} \bar{u} \\ \bar{v} \end{pmatrix} = R_\delta \begin{pmatrix} \bar{u} \\ \bar{v} \end{pmatrix} \quad (1)$$

where, R_δ is identified with the counterclockwise Oz-rotation matrix. The magnetic declination, δ=20º50'W (–20.833º) was obtained from NOAA National Geophysical Data Center calculator (http://www.ngdc.noaa.gov/geomagmodels/Declination.jsp).

Despite of the fact that wind components have changed due to the magnetic declination correction, the magnitude of the wind velocity is kept unchanged. The tanθ (ratio between the components) has an increment straight in the argument. Therefore, it is enough to sum δ to the old angle ($\theta'=\theta+\delta=\theta$-20.883º). Besides, the correction for the magnetic declination, wind direction time-series, showed a systematic difference amongst the aerovanes. This is probably due to some aerovanes being a little misaligned. In fact, after subtracting the mean value of each aerovane and summing the overall averaged direction, all aerovane direction becomes consistent with each other (Fig. 3). The ten-minute mean amplitude of wind direction along the Murici II Campaign is relatively large, reaching almost 80º by the day of year 266. Note that even after correction, a random variability

Table 1. Basic averaging methods of the observations. All mean values were taken over a 10-min time interval.

$V_S = \frac{1}{N}\sum_n S_n$	Scalar mean wind speed (observed)
$\bar{u} = \frac{1}{N}\sum_n -S_n \sin\theta_n$	Zonal mean wind component
$\bar{v} = \frac{1}{N}\sum_n -S_n \cos\theta_n$	Meridional mean wind component
$\bar{\theta} = \tan^{-1}\frac{\bar{u}}{\bar{v}}$	Vector mean wind direction
$V_R = (\bar{u}^2 + \bar{v}^2)^{\frac{1}{2}}$	Vector mean wind speed
$I = \frac{\sigma_n}{S_n}$	Turbulence intensity
$G_n = \frac{S_{pn}}{V_S}$	Gust factor, is a 10-min peak velocity
$A_n = S_{pn} - V_S$	Gust Amplitude

of up to 10º still remains. It is observed that in the two days of the campaign (DOYs 267 and 268) the variability of wind direction has decreased.

Maximum and minimum instantaneous wind speeds were taken from each ten-minute intervals and were averaged hourly for each aerovane and then averaged over all ten aerovanes. Turbulence intensity (standard deviation over mean wind speed), gust factor (maximum wind speed over mean wind speed), and gust amplitude (maximum wind speed minus mean wind speed) were computed from the available dataset. Since the aerovane sampling rate is 0.5Hz, the time interval between two consecutive readings is two seconds and, thus, the gust we consider here has automatically a time width of two seconds. It seems that there is not a standard in defining the duration of the gust. Usually the gust duration is defined as a function of instrumentation/data availability or specific objectives and two or three seconds wind peak in a time-interval of ten minutes is often used.

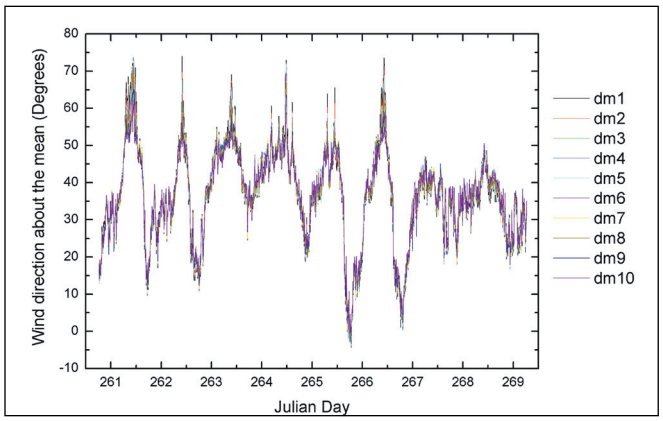

Figure 3. Direction time series after correction for magnetic declination and for offsets. The symbol 'dm' means mean direction of each aerovane.

Sonic anemometer and aerovane at 1.5-m height

We also considered in this analysis data from a sonic anemometer and aerovane at 1.5-m height. They were close to each other about 2m and about 20m apart from the aerovane mesh. They were operated at the same sampling rate as the aerovanes of the mesh, but in this case the raw data were stored. These dataset allowed us to carry out a more refined spectral analysis, which would not be possible with the ten-minute averaged mesh data.

ESTIMATING σ_y^2 AS INPUT FOR DISPERSION MODELS

One of the most common dispersion models is the Gaussian plume, as described in Hanna *et al*. (1982); Seinfeld and Pandis (1999) and Arya (1999). To apply the Gaussian model, the ground surface should be relatively homogeneous so that the calculation of the statistical properties at a given position can be used at other ones. The main statistical parameter to be determined from observations is the mean wind (easy task) and the lateral (σ_y^2) and vertical (σ_Z^2) variances (tough task). Conceptually, these variances can be determined from observing the diffusion of a point source, for example, and measuring the concentration with a fast response device. Then, one computes the mean value and the variance of concentration for a suitable averaging time, usually ten minutes. The difficulty in this procedure is that to get known the spatial variation of the variances, an array of devices must be setup, which is often not possible. Furthermore, measurements in real time provide a diagnostic of the concentration, instead a prognostic as is usually desirable.

In the modeling study of dispersion over the CLA area carried out by Moreira *et al*. (2011), σ_y^2 is expressed in terms of an empirical formula that depends on many unknown parameters in practice, such as the convective velocity scale and the Obukhov length. Both are not measured in a regular basis, and, besides, they are related to the unstable condition of the surface layer, a condition not clearly satisfied in the CLA area. For instance, Magnago *et al*. (2010) found that 93% of data collected in August, 1999 (beginning of dry season) lie to the stability parameter interval of $-0.3 < z/L < 0.1$. Thereby, the use of σ_y^2 as it is provided by the statistical model of diffusion (Hanna *et al*., 1982; Arya, 1999), instead of semi-empirical formulas, would be more reliable, with the advantage that wind speed and direction are measured routinely in the CLA. According to Taylor's approach (Arya, 1999), σ_y can be obtained from σ_V by means of the Lagrangian autocorrelation function, as in Eq. 2:

$$\rho(t_0,\zeta) = \frac{\overline{v'(t_0)\,v'(t_0+\zeta)}}{\sigma_v^2} \qquad (2)$$

where, $\xi = t - t_0$. In the case of a stationary flow, the starting time is not important and the autocorrelation can be expressed only as a function of ξ Lateral concentration variance is then given by Eq. 3 (Hanna *et al*., 1982; Arya, 1999):

$$\sigma_y^2(t) = 2\sigma_v^2 \int_0^t \int_0^{t'} \rho(\zeta)\, d\zeta dt' \tag{3}$$

Taylor (1921) assumed an exponential form for $\rho(\xi)$, although another form, $\exp(-ct^2/\tau_L)$ has been suggested as well (Arya, 1999). The latter form seems not to fit our observations, because the rounded shape close to $\xi = 0$ is not observed. We thereby adopt the simple form assumed by Taylor: $\rho(\xi) = \exp(-\xi / \tau_L)$, where τ_L is the Lagrangian time scale. Therefore, the concentration variance will be given by Eq. 4:

$$\sigma_y^2 = 2\sigma_v^2(t)\,\tau_L^2\left[\frac{t}{\tau_L} - 1 + \exp\left(-\frac{t}{\tau_L}\right)\right] \tag{4}$$

Two well-known limit cases, also found by Taylor (1921), are: for $t << \tau_L$; in this case, the autocorrelation function is close to the unit ($\rho \approx 1$). And, for $t >> \tau_L$, when the $\rho \to 0$. The Lagrangian concentration variance within this limit case can be written as in Eq. 5:

$$\sigma_y^2(t) \approx \begin{cases} \sigma_v^2 t^2 & \text{for } t \ll \tau_L \\ 2\sigma_v^2 \tau_L t & \text{for } t \gg \tau_L \end{cases} \tag{5}$$

All those parameters refer to a Lagrangian system of coordinates. Actual measurements are carried out at a fixed point (Eulerian coordinates). There is no general exact procedure for obtaining Lagrangian coordinates from Eulerian coordinates or vice-versa in a turbulent flow. To do this, we will make use of a heuristic approach based on Hanna *et al*. (1982), but somewhat modified. Consider a turbulent eddy as a circulating vortex of radius R in a flow approaching an anemometer with mean speed U. A particle at the edge of the eddy will have a tangential velocity, whose OY-component is v. The time for the particle to perform the entire eddy in the OY direction is a measure of the Lagrangian time-scale, being equal to $2R/v$. On the other hand, for the anemometer to capture the entire eddy, it will take a time given by $2R/(U+u)$, where u is OX component of the eddy tangential velocity. Thus, the ratio τ_L/τ_E for one single eddy will be something of the order of $(U+u)/v$. If we take into account a large range of eddies in average (using the same time-interval to compute $U=\bar{u}$), we can estimate Lagrangian-to-Eulerian time-scale ratio as Eq. 6:

$$\beta \equiv \frac{\tau_L}{\tau_E} = \frac{\sigma_u}{\sigma_v} \tag{6}$$

Note that the σ_u and σ_v, which appear in the previous equation, are the Eulerian standard deviations, that is, they are measured in a fixed frame of reference.

RESULTS AND DISCUSSION

Wind characteristics

The diurnal cycle of wind direction averaged over all aerovanes is strongly marked var-ying from 25 to 55º, that is, on the central half of the first quadrant. Its peak value occurs at about 1000 LST. (Fig. 3). Scalar and vector mean wind speed (not shown) are very close throughout the time-series, and the maximum mean difference for the diurnal cycle is not greater than about 2%. Such wind persistence is a characteristic of trade winds and already a known fact for a much larger area covering the CLA site. Hereafter, we will then refer only to the vector mean wind speed in the following discussion. Figure 4 shows ten-minute time-series for the magnitude of the vector mean velocity and the spatial average over them. A not negligible variability is observed among the aerovanes, it is not clear its origin. A misalign-ment of aerovanes would generate systematic differences between each couple of aerovanes. We have investigated those differences, and found that they are either negative or positive throughout the time-series, i.e., no systematic difference was found. Therefore, a misalign-ment does not seem to be the answer. Furthermore, this large scattering is also observed in the scalar wind speed and suggests a length-scale of few meters.

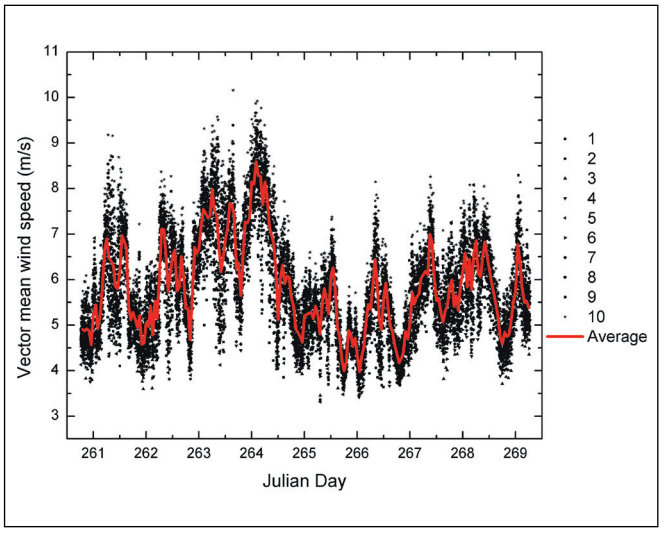

Figure 4. Aerovane mesh-min averaged time series. Red line is the spatial average, and black symbols, individual aerovane values.

Figure 5 presents the vector mean wind speed, maximum and minimum wind, and direction averaged over all days and over all aerovanes. We have applied offsets of -3 and + 3m/s to the maximum and minimum speed, respectively, in order to enhance the diurnal cycle on the graphic. Mean wind speed presents values ranging from 5.0 to 6.5m/s. Minimum and maximum wind speed are about 3.0 and 9.0m/s, respectively. These numbers show that wind is rather strong in the CLA site. The main contribution comes from the trade winds, whereas the variation along the diurnal cycle is due to the mesoscale regime of the land-sea breeze circulation, which strengths the wind during the daytime and weakens it during nighttime.

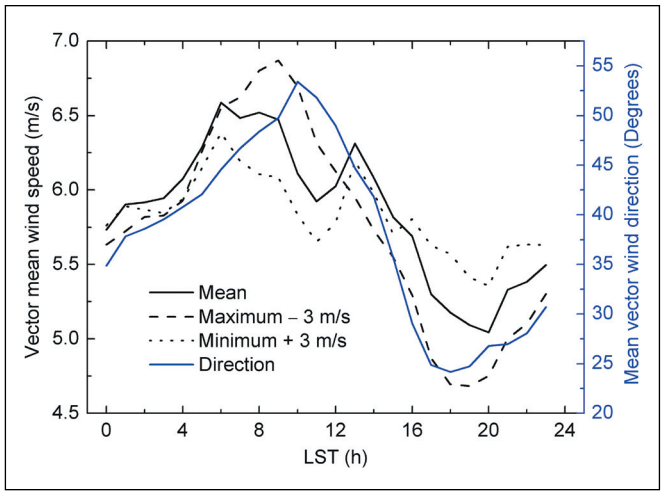

Figure 5. Diurnal cycle of mean wind, maximum and minimum wind, and wind direction.

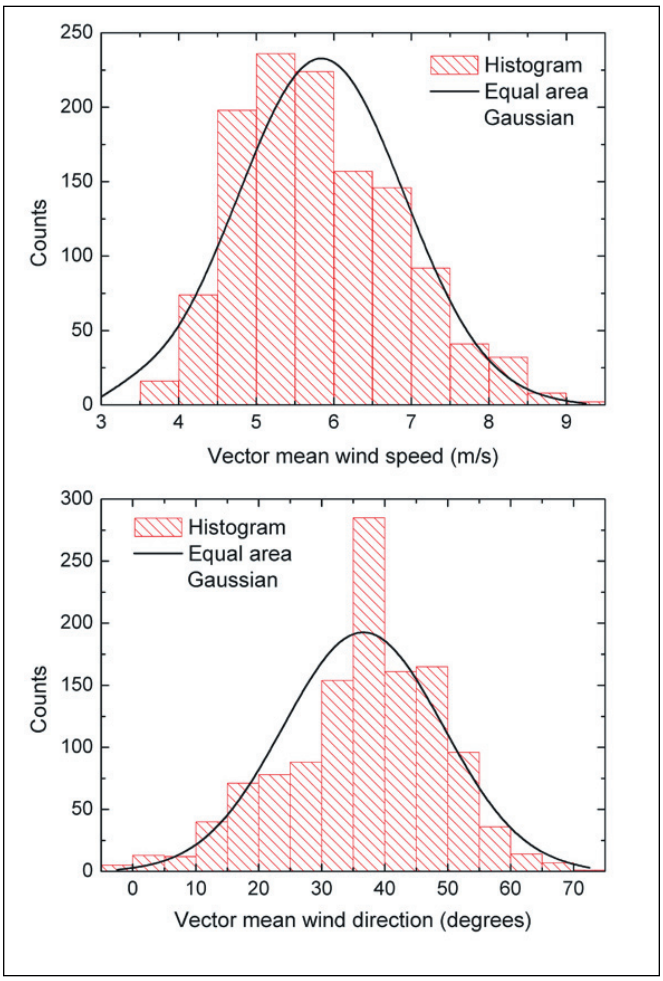

Figure 6. Distribution of the vector mean wind speed (above) and the vector mean wind direction (below) with their correspondent normalized Gaussian curve. Wind speed trends to be below the mean value (skewness=0.51) and wind direction trends to be above the mean value (skewness = –0.45).

To complete the statistical characterization of the wind, histograms for the mean wind speed and the wind direction for the whole time series after averaging for the ensemble of all ten aerovanes were drawn in Fig. 6. Accordingly, the wind average and standard deviation are 5.8 and 1.0 m/s, respectively. For direction, average and standard deviation are 36.6º and 12.4º, respectively. Gaussian distributions based on those values have also been plotted. As it can be seen, both wind speed and direction are not symmetrically distributed about the mean value; wind speed tends to be below the mean value (skewness = 0.50) and wind direction tends to be above the mean value (skewness = –0.43).

Gust and turbulence features

There are still very few studies of the impact of wind on the rocket and launch tower in the Brazilian space program. Wind engineering has devoted most studies to other kind of structures, such as transmission line towers or tall buildings. Even if the results for transmission line were extended to other vertical structures like a rocket or a launch pad, the particular features found in the CLA would likely fall out the code criteria. Gusts can affect rocket structure due to stresses caused either because of the strength or because of the frequency of the gusts (Hrinda, 2009). A particular concern is about the structure natural frequency, which may not withstand to resonance.

Turbulence intensity (standard deviation over mean wind speed), gust factor (maximum wind speed over mean wind speed), and gust amplitude (maximum wind speed minus mean wind speed) were computed from the available dataset (Table 1). Time-series show that the gusts and turbulence are intensified between 0800 and 1300 LST, likely due to the interaction between the sea breeze and the Trades

(Fig. 7). Turbulence intensity, gust factor, and gust amplitude are strongly correlated to each other: their peak values take place at about 1000 LST. Turbulence intensity is mainly associated with the wind shear, and its value is between 0.13 and 0.27. This value can validate wind tunnel simulations by Pires *et al*. (2009), who obtained a turbulence intensity of about 0.20 along a stream wise distance of 200m from the cliff. In fact, the mesh is closer than the cliff, ~100m, and for this distance the value obtained by Pires *et al*. (2009) is about 0.15. Gust factor and gust amplitude are between 1.3 and 1.8m/s, and 2.2 and 4.3m/s, respectively. This kind of comparison will be very important in the ongoing research, in order to find relationships between results from wind tunnel and field experiment.

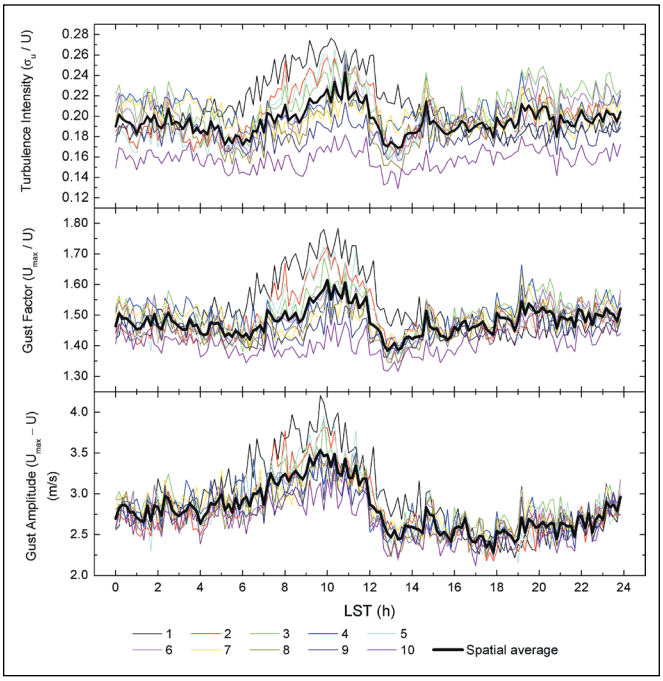

Figure 7. Diurnal cycle of turbulence and gust properties.

Figure 8 shows how the ensemble averaged ten-minute gust factor found in the CLA is distributed with respect to Adelfang *et al*. (2008) curve, who present a set of formulas supported in the literature to compute ten-minute gust factors for a range of heights (10 to 150m) and a range of peak winds (4.6 to 15.4m/s), based on the reference wind at 18.3m (60ft). Their results show a consistent gust factor decrease as the wind peak or height increases. At 10m, their maximum gust factor value is about 1.87 and a minimum value of 1.62, corresponding to the mean wind speeds of 2.5 and 9.5m/s, respectively. An extrapolation of such formula predicts a minimum gust factor of 1.6. This corresponds, indeed, to the maximum gust factor we have found.

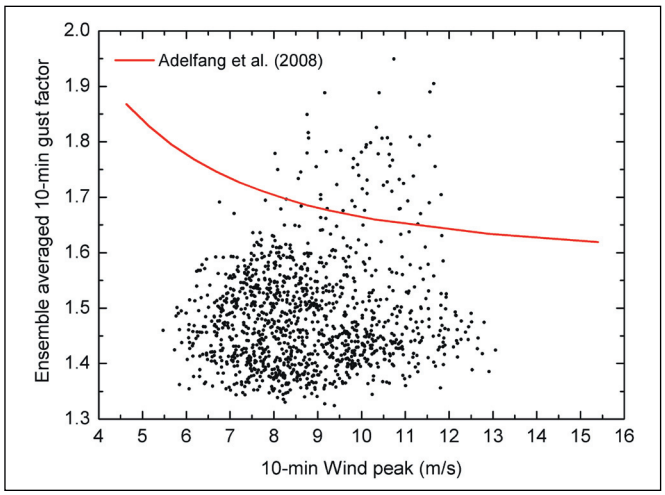

Figure 8. Comparison of CLA gust factors with Adelfang et al.'s empirical formula.

The compilation of Adelfang *et al*. (2008) shows that, for wind peaks greater than 15m/s, the gust factor increases asymptotically with respect to the averaging time, there not being any difference between five and ten-minute averaging within 0.1% error. Other quantity that has been used to model wind peaks is the gust amplitude, defined as $A = u_{max} - u$, in which u_{max} is the ten-minute wind peak and u the mean wind in the same time interval. This is used particularly to model the vertical wind profile, and a gust amplitude of 6m/s nearby the ground has been reported.

One important issue that should be tackled in the Brazilian space program is the planning of more laboratory and field experiments to characterize not only the flow regime in the CLA, but also to better understand how such a flow regime can affect launches as well as the rocket and launch tower structures themselves. The lack of acceptance criteria for wind conditions makes more difficult the use of existing data. As Adelfang *et al*. (2008) point out: "there is not a clear precedent from building codes to follow in recommending design risk for a given desired lifetime of structure." In this way, the simple usage of already existing building codes can be misleading.

Nondiurnal cycles

Despite the fair weather along the field campaign, some variation in the surface pressure field has been observed between DOYs 263 and 265 suggesting a wave-like perturbation modulating the pressure oscillation, but not its amplitude (Reuter, 2011). According to the wind time-series a high pressure system should be placed over the ocean, causing an acceleration of the flow inland. Frequency-domain analysis

(Fig. 9) reveals the presence of non-diurnal cycle forcings. The main peaks take place at 0.25, 1.0, 2.0, and 3.0 day^{-1}, corresponding to periods of four days, one day, 12 hours, and 8 hours, respectively.

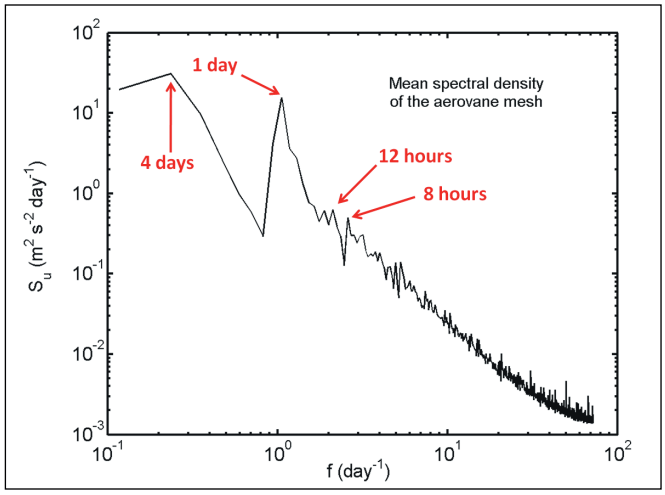

Figure 9. Averaged spectrum of the aerovane mesh. Frequencies of 0.25 and 1.0 day^{-1} are well apparent. Higher frequencies seem to be present, but not clear.

The averaged autocorrelation of the mesh data (not shown) is consistent with a diurnal cycle and another cycle of about four days, probably due to a large-scale system or still due to the limited length of the series. Those cycles are apparent in the frequency-domain representation (Fig. 9). The spectrum presents some higher frequencies with a time scale of 8 to 12 hours, which may be associated with the double-peak diurnal cycle of surface pressure *(barotropic tide)*. However, they have low strength and are not clear enough in the spectrum. Surface pressure data supportthe scenario of a forcing of larger spatial scale acting. For instance, the surface pressure variation analyzed by Reuter *et al*. (2011) by means of Wavelet Transform in the same period of Murici II Campaign shows a period lying from 10 to 14h, consistent with what we have found from Fast Fourier Transform (FFT) applied to the wind data. The little difference (~2 h) between wind and pressure spectra may be due to the dynamics process itself, however we did not go through this question.

Higher sampling rate data: diffusion parameters

A 2-D sonic anemometer was placed close to an aerovane and it was operated during about the same time as the Murici II Campaign. Five DOYs from 264 to 269, 2008, were analyzed. Data from both measurements were recorded every 2s (0.5-Hz sampling rate), allowing a more detailed analysis of the wind statistics. We compared the performance between the anemometers, especially to assess the aerovane response to rapid variations of the wind.

A similar study by Fisch (2010) deployed a sonic anemometer and an aerovane on 10-m high masts, showing that differences between them are rather small, being $U_{sonic} - U_{aerovane} = 0.3$m/s, regardless the average, it is performed for one or ten minutes.

In order to study the statistical wind properties applied to dispersion problems, they have to be considered with respect to the direction along to the prevalent wind, which we called *Ox* (wind component in this direction will be called *u*: longitudinal component) and the direction across it, *Oy* direction (wind component will be called *v*: lateral component). Here after throughout this subsection, *u* and *v* will mean longitudinal and lateral wind components, respectively, instead of zonal and meridional wind components. Since wind changes direction all the time, we considered the prevalent wind direction the time-averaged value over a time-interval Δt and, therefore, $\bar{u}(\Delta t) = U$ and $\bar{v}(\Delta t) = 0$. We have varied Δt from 1.5 minutes to five days and took the mean value: for example, there are 960 time-intervals of 7.5 minutes in five days, then the mean ρ is calculated as $\sum \rho_k$ / 960; for Δt=1 day we have $\rho = \sum \rho_k$ / 5; for Δt=5 days we have just $\rho = \rho_k$ / 1. A common behavior observed in the autocorrelation function is that after a large enough lag it becomes negative. To compute the integral time scale we used only non-negative values of auto correlation function.

Figure 10 shows the autocorrelation coefficient computed for several time intervals (= 5 days, 1 day, 12h, 6h, 2h, 1h, 30min, 10min, 7.5min, and 1min). Note that for the greatest time intervals the autocorrelation no longer approaches zero until 1-min lag. However, time-intervals of 12 hours to 5 days show an approaching to zero when longer lags are considered. For example, for a one-day time-interval, the curve crosses the abscissa only at a time-lag of about 5h. This shows that larger scales motions are captured by the autocorrelation function, but only when the plots are extended to longer time lags they become apparent. For instance, when the autocorrelation function for the time interval of five days like seen in Fig. 10 (continuous black line) is plotted for a time-lag as longer as the time interval considered oscillations about zero showing the diurnal cycle can be seen. Thereby, what is seen in Fig. 10 for the time lag up to 60s is the turbulence correlation superposed (or modulated) by larger scale motion. On the other hand,

when shorter time-intervals are taken into account, the largest motion scales are filtered out and then the autocorrelation function carries information of the turbulence only. Figure 10 shows a significant difference between the series of 24-h time-interval (continuous red line) and a series of 2-h time-interval (continuous navy line). The former attains cross the abscissa at 5h, whereas the latter cross the abscissa for a time lag of about 40 minutes. The shortest time-interval plottedis of 1.5min, which cross the abscissa at 12s approximately.

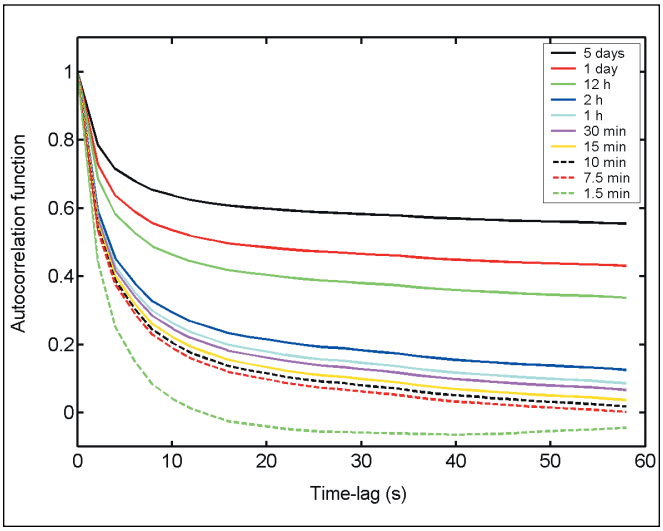

Figure 10. Sonic-anemometer autocorrelation function plotted up to the time-lag of 60s.

Integral time-scale was obtained from wind measured in an Eulerian frame of reference, therefore, it is a Eulerian time-scale. To transform it into Lagrangian time-scale we use Eq. 6. The variation of the number β in relation to the time-interval is shown in Fig. 11. β was computed for sonic anemometer and aerovane. Aerovane presents systematic lower values. Usually for use in dispersion model sonic anemometer data are desirable because of their faster response to wind changes, but aerovanes are more commonly used for monitoring winds in the CLA as elsewhere. Thereby, to check its response and the wind properties measured by aerovanes were important points in the present analysis. The integral time-scale ratio (β) for short lags varies from about 1.1 (aerovane) to 1.3 (sonic). The maximum value is 1.55 (sonic) for a lag as long as five days (whole time-series). It can be noticed from Fig. 11 that β is not a parameter that will affect significantly the integral time-scale. Based on this, we present in Fig. 12 the integral time-scale of u- and v-component only for Lagrangian case. Time-scale was computed by integrating the autocorrelation curves in Fig. 11 until the first zero.

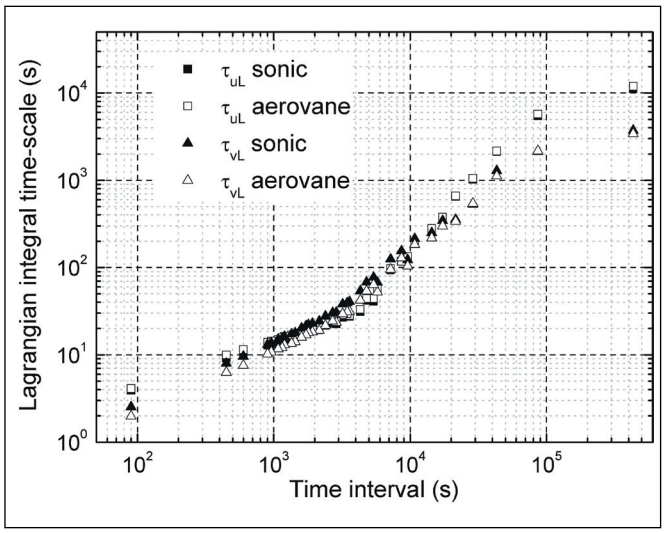

Figure 11. Lagrangian integral time-scale: the subscript refers to the components u (longitu-dinal) or v (lateral).

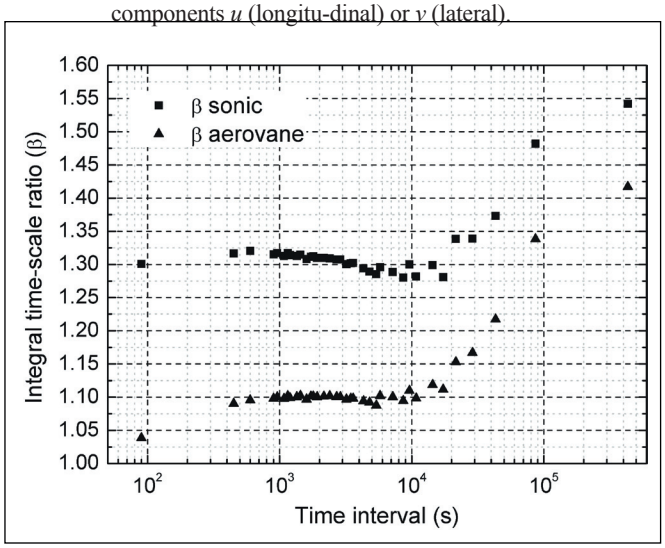

Figure 12. Time-scale ratio of Lagrangian and Eulerian frames of reference.

The relationship between dimensionless Lagrangian lateral standard deviation [σ_y /(σ_v τ_{vL})] and the dimensionless time [t /τ_{vL}] for a time-interval of 10-min is shown in Fig. 13. The choice of ten minutes average time for representing the Lagrangian standard deviation is based on the fact that this is the most usual averaging time employed in Meteorology and in dispersion studies in particular. A similar plot for the Eulerian σ_y (not shown) cannot be distinguished by eye given the closeness of them. For the particular case of the CLA, where wind has a strong persistence, it seems reasonable to use the Eulerian variances to input dispersion Gaussian models. In

situation with low wind and/or presence of obstacles nearby, the scenario can be rather different.

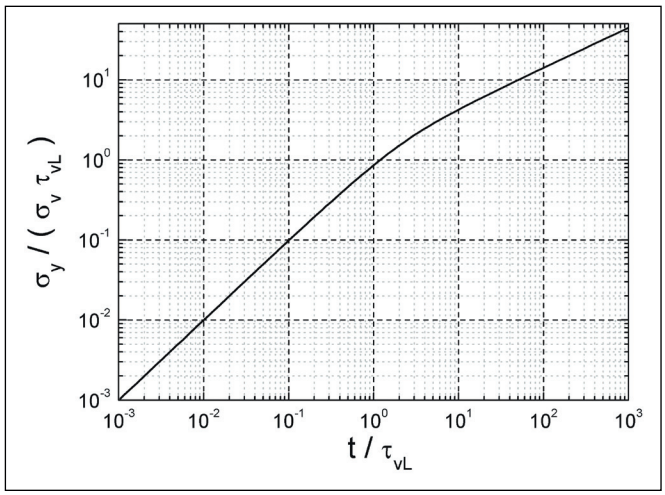

Figure 13. Standard deviation of the concentration in the lateral direction, assuming an exponential decay of the autocorrelation function. The Eulerian and Lagrangian are undistinguishable by eye. Two main behaviors can be seen: for $t<\tau_v$, σ_y increases as t, and for $t>4\tau_v$, σ_y increases as $t^{1/2}$.

CONCLUSIONS

This study aimed at better understanding processes governing the wind regime in the CLA and at developing tools for analyzing the impact of wind on rocket structure and on the dispersion of pollutants released during the launch. We presented data of wind and turbulence collected in the CLA during a ten-day field experiment in the dry season of 2008. Wind speed, wind direction, turbulence intensity, gust factor, and gust amplitude present a marked diurnal cycle. Vector mean wind speed, minimum speed, and maximum speed are about 6.0, 3.0 and 9.0m/s, respectively. Mean wind direction is about 40º. The gust factor found for CLA (1.5 in average) is rather low when compared with literature (1.6 to 1.9). Spectral analysis of aerovane mesh shows two strength frequencies (0.25 and 1 day^{-1}) and two lower strength frequencies (2 and 3 day^{-1}). The lowest frequency may be associated with a large-scale system, while the 1 day^{-1} frequency is obviously associated with diurnal cycle. The two higher frequencies may be associated with the pressure diurnal cycle, which reaches two peaks a day due to the barotropic tide.

The concern with pollutant dispersion and environmental impact reports lead us to investigate more direct methods to estimate diffusion parameters, such as integral time-scale, standard deviation of concentration, and relationships between Lagrangian and Eulerian frames of reference. This last task, which should be deeply studied, is very import since model's diffusion parameters are Lagrangian quantities whereas measurement are usually Eulerian quantities. The time-series we analyzed so far is still short for drawing general statements. In a future work, we would analyze longer time-series. Nonetheless, the dispersion parameters we have computed may be applied to dispersion models eventually for those days of year when they were collected or in general studies considering that the series length is short and may be not representative of other days of year. Finally, the characterization of general wind behavior and turbulence within the surface boundary layer must be a central concern in the CLA to guarantee the safety of the launching operations.

ACKNOWLEDGEMENTS

The authors thank J. Yamasaki for helping with data and metadata. The authors also thank the *Fundação de Amparo à Pesquisa do Estado de São Paulo* (FAPESP) under Grant number 2010/16510-0 and the *Conselho Nacional de Desenvolvimento Científico e Tecnológico* (CNPq) under Grant Universal 471143/2011-1, PQ 303720/2010-7, and the Project 559949/2010-3 for supporting this study.

REFERENCES

Adelfang, S. *et al*., 2008, "Winds, in Terrestrial environment (climatic) criteria guidelines for use in aerospace vehicle development 2008 revision", NASA technical memorandum 4511 (Johnson D.L., editor), Chap. 2.

Arya, S.P., 1999, "Air pollution meteorology and dispersion", Oxford University Press, New York, 310 pp.

Decker R.K., Leach R., 2005, "Assessment of atmospheric winds aloft during NASA Space Shuttle Program day-of-launch operations", American Institute of Aeronautics and Astronautics (AIAA).

Decker R.K., Barbré Jr., R.E., 2011, "Quality control algorithms and proposed integration process for wind profilers used by launch vehicle systems", 15th Conference on

Aviation, Range and Aerospace Meteorology of the American Meteorological Society (AMS), Los Angeles, 2011.

Fisch, G., 1999, "Características do perfil vertical do vento no centro de lançamento de foguetes de Alcântara (CLA)", Revista Brasileira de Meteorologia, Vol. 14, No. 1, pp. 11-21.

Fisch, G., 2010, "Comparisons between aerovane and sonic anemometer wind measurements at Alcântara Launch Center", Journal of Aerospace Technology Management, Vol. 2, No 1, pp. 105-110.

Gisler, C.A.F. *et al*., 2011, "Análise estatística do perfil de vento na camada limite superficial no centro de lançamento de Alcântara", Journal of Aerospace Technology Management, Vol. 3, No. 2, pp. 193-202.

Hanna, S.R. *et al*., 1982, "Handbook on atmospheric diffusion", U.S. Department of Energy Technical Report, 102 pp.

Hrinda, G.A., 2009, "Single-point-attachment wind damper for launch vehicle on-pad motion", NASA Langley Research Center, Technical Report.

Kingwell, J. *et al*., 1991, "Weather factors affecting rocket operations: a review and case history", Bulletim of the American Meteorological Society, Vol. 72, pp. 778-793.

Magnago, R. *et al*., 2010, "Análise espectral do vento no Centro de Lança-mento de Alcântara (CLA)", Revista Brasileira de Meteorologia, Vol. 25, No.2, pp. 260-269.

Moreira, D.M. *et al*., 2011, "A multilayer model to simulate rocket exhaust clouds", Journal of Aerospace Technology Management, Vol. 3, No. 1, pp. 41-52.

Pires, L.B.M. *et al*., 2009, "Studies using Wind Tunnel to Simulate the Atmospheric Boundary layer at the Alcântara Space Center", Journal of the Aerospace and Technology Management, Vol. 1, No. 1, pp. 91- 98.

Reuter, E., 2011, "O desempenho do modelo ETA: uma análise comparativa do vento entre medições in situ e o modelo para o Centro de Lançamento de Alcântara", Tech. Report, related to the CNPq Ph.D. program at the Instituto de Pesquisas Espaciais (INPE), agosto, 2008, 14 pp.

Taylor, G.I., 1921, "Diffusion by continuous movements", Proceedings of the London Mathematical Society, Vol. 2, pp. 196-211.

Seinfeld, J.H, Pandis, S.N., 2006, "Atmospheric Chemistry and Physics", John Wiley & Sons, Inc., New Jersey.